



# Phase coexistence in proton glass

Authors: V.Hugo Schmidt, Z. Trybula, N.J. Pinto, and S.M. Shapiro

This is an Accepted Manuscript of an article published in [Phase Transitions](#) on [date of publication], available online: <http://www.tandfonline.com/10.1080/01411599808227666>.

V.H. Schmidt, Z. Trybula, N.J. Pinto, and S.M. Shapiro, "Phase coexistence in proton glass," *Phase Transitions* 67, 499-520 (1998).

Made available through Montana State University's [ScholarWorks](http://scholarworks.montana.edu)  
[scholarworks.montana.edu](http://scholarworks.montana.edu)

# PHASE COEXISTENCE IN PROTON GLASS

V.H. SCHMIDT<sup>a,\*</sup>, Z. TRYBULA<sup>b</sup>, N.J. PINTO<sup>c</sup>,  
and S.M. SHAPIRO<sup>d</sup>

<sup>a</sup>Physics Department, Montana State University, Bozeman, MT 59717, USA; <sup>b</sup>Institute of Molecular Physics, Polish Academy Science, Poznan, Poland; <sup>c</sup>Department of Physics and Electronics, U. Puerto Rico, Humacao, PR 00661, USA; <sup>d</sup>Physics Department, Brookhaven National Laboratory, Upton, NY 11973, USA

(Received September 1997)

Proton glasses are crystals of composition  $M_{1-x}(NW_4)_xW_2AO_4$ , where  $M = K, Rb, Cs$ ,  $W = H, D$ ,  $A = P, As$ . For  $x=0$  there is a ferroelectric (FE) transition, while for  $x=1$  there is an antiferroelectric (AFE) transition. In both cases, the transition is from a paraelectric (PE) state of tetragonal structure with dynamically disordered hydrogen bonds to an ordered state of orthorhombic structure. For an intermediate  $x$  range there is no transition, but the hydrogen rearrangements slow down, and eventually display nonergodic behavior characteristic of glasses. We and others have shown from spontaneous polarization, dielectric permittivity, nuclear magnetic resonance, and neutron diffraction experiments that for smaller  $x$  there is coexistence of ferroelectric and paraelectric phases, and for larger  $x$  there is coexistence of antiferroelectric and paraelectric phases. We present a method for analytically describing this coexistence, and the degree to which this coexistence is spatial and/or temporal. We discuss also the experimental determination of these coexistence parameters.

*Keywords:* Phase transition; Ferroelectric; Antiferroelectric; Glass

## INTRODUCTION

A proton glass is a crystal in which the protons dynamically occupy disordered positions in hydrogen bonds, and freeze into these disordered positions as temperature decreases. The prototypical proton

---

\* Corresponding author.

glass, discovered by Courtens (1982), is  $\text{Rb}_{1-x}(\text{NH}_4)_x\text{H}_2\text{PO}_4$  (RADP). Other proton (or deuteron) glasses have K or Cs for Rb, As for P, and/or D for H. We briefly review some structural features of proton glass and its parent crystals.

Proton glass retains its room temperature body-centered tetragonal structure down to the lowest temperatures. The dielectric permittivity increases with decreasing temperature according to a Curie–Weiss law, but then decreases to a small temperature-independent value with considerable frequency dispersion as temperature decreases further. The dielectric loss shows a corresponding dispersion. There is no thermodynamic phase transition from the paraelectric (PE) to the proton glass (PG) phase, but we and others refer to these as separate phases for reasons which are discussed later.

One parent crystal of proton glass is  $\text{RbH}_2\text{PO}_4$  (RDP), which undergoes a second-order ferroelectric (FE) phase transition at  $T_c = 147\text{ K}$  in which the hydrogens in the  $\text{O}-\text{H}\cdots\text{O}$  bonds arrange themselves into ordered off-center positions in these bonds (Jona and Shirane, 1962). The transition is accompanied by a structural change from a body-centered tetragonal  $\text{I}\bar{4}2\text{m}$  unit cell with  $\mathbf{c}$  the preferred axis, to a double-sized face-centered orthorhombic  $\text{Fdd}$  unit cell with the  $\mathbf{a}$  and  $\mathbf{b}$  axes rotated  $45^\circ$  about  $\mathbf{c}$ . The spontaneous polarization  $P_s$  which develops along  $\mathbf{c}$  rises sharply below  $T_c$  and soon levels off to a saturation value. The permittivity  $\epsilon_c$  along the  $\mathbf{c}$  axis obeys a Curie–Weiss law, becoming very large as  $T_c$  is approached from above. Below  $T_c$  it remains fairly large over a range of tens of degrees because of domain wall response. The permittivity along  $\mathbf{a}$  obeys a different Curie–Weiss law with a lower Curie–Weiss temperature, so it remains fairly small (of order 100) even at  $T_c$ . Below  $T_c$  it drops rapidly to a low, temperature-independent, value, because it is unaffected by domain wall displacement.

The other parent crystal is  $\text{NH}_4\text{H}_2\text{PO}_4$  (ADP), which undergoes a strongly first-order antiferroelectric (AFE) transition at  $148\text{ K}$  in which the hydrogens order in a different manner (Känzig, 1957). The unit cell keeps the same orientation and nearly the same size, but becomes orthorhombic  $\text{P}2_12_12_1$  and loses the body center Bravais lattice point. Both the  $\mathbf{a}$  and  $\mathbf{c}$  axis permittivities behave similarly to the  $\mathbf{a}$  axis permittivity for RDP, above the respective transition temperatures of these crystals.

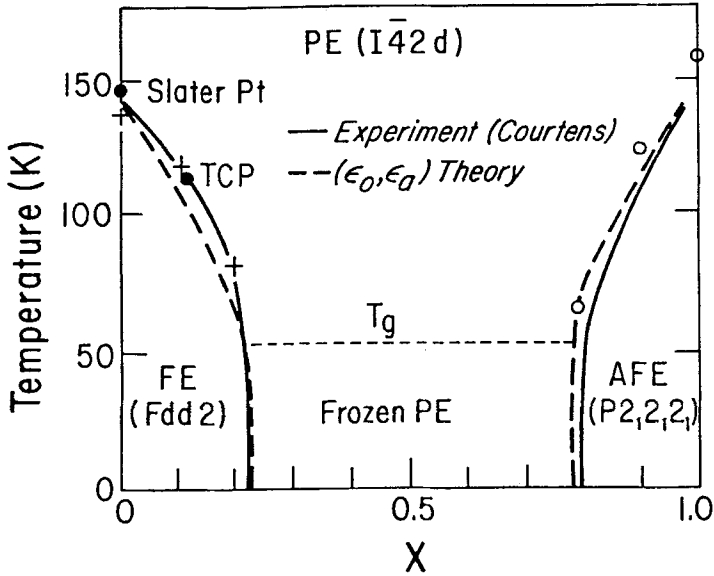


FIGURE 1 Phase diagram for RADP (Schmidt, 1987) showing boundaries determined by experiment, by theory, and by Monte Carlo heating (crosses) and cooling (circles) runs.

Two reviews of proton glass behavior provide the phase diagram for RADP (Schmidt, 1987) shown in Fig. 1, and the specific range over which RADP crystals exhibit proton glass behavior without coexistence, namely  $x=0.22$  to  $x=0.74$  (Courten, 1987). Lack of coexistence is signaled by lack of a permittivity cusp; compare Fig. 2(d) with Figs. 2(a)–(c) in which cusps do appear. For  $x$  values outside this range, it is possible to observe effects of phase coexistence of the PE or PG phase with the FE phase (for small  $x$ ) or with the AFE phase (for large  $x$ ). The purpose of this paper is to examine this coexistence. First we describe the evidence for coexistence. Then we present a method for describing the temporal and spatial nature of this coexistence. We conclude with a discussion of unsolved problems regarding coexistence.

## EXPERIMENTAL EVIDENCE FOR COEXISTENCE

We will present evidence from neutron diffraction, from spontaneous polarization in conjunction with dielectric permittivity, and from

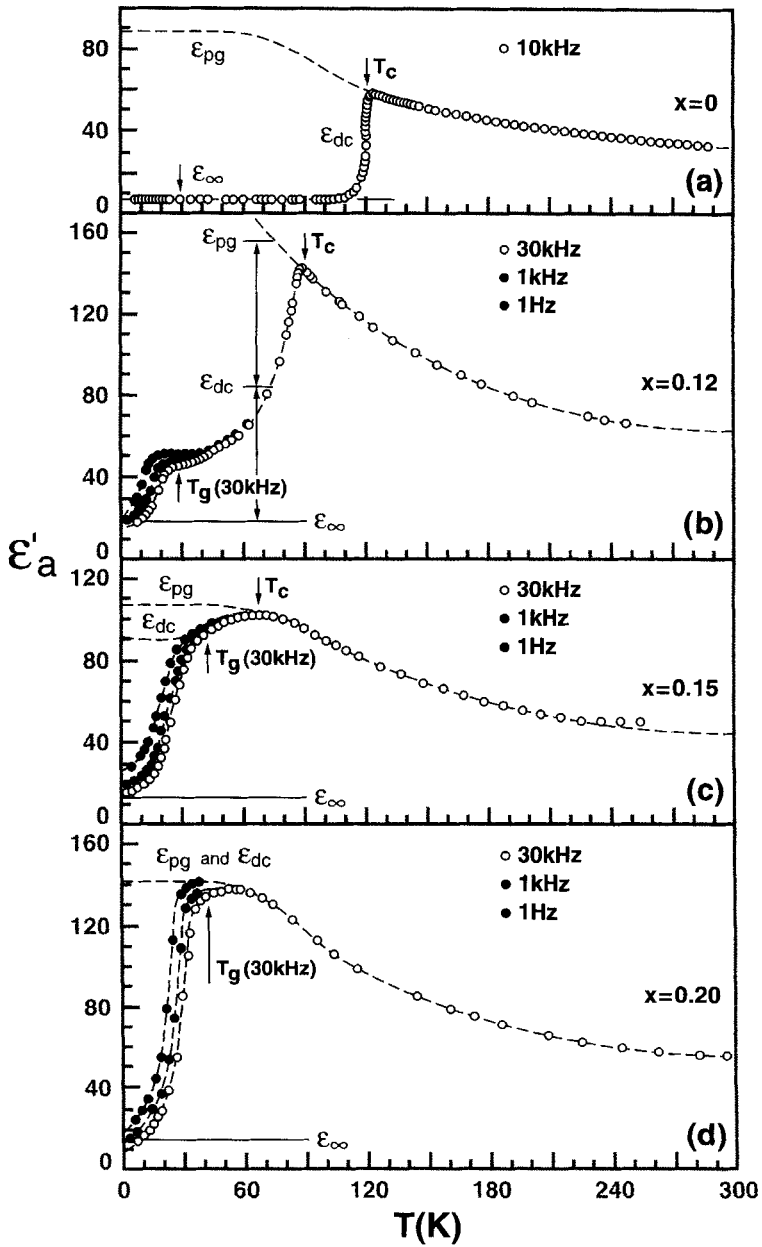


FIGURE 2 Temperature dependence of the real part of the a axis dielectric permittivity for RDA and three RADA crystals (adapted from Trybula *et al.*, 1991).

nuclear magnetic resonance (NMR) for coexistence of the FE and PE phases. For AFE/PE coexistence we have neutron, dielectric, and NMR evidence. Finally, field cooling/zero field heating experiments show coexistence of the PG and PE phases.

Neutron diffraction provides clear evidence for coexistence, because the Bragg reflections for both the PE and FE (or AFE, depending on  $x$ ) phases are seen over a temperature range of width of order 10 K (Schmidt *et al.*, 1996). Each (hk0) Bragg spot divides into four FE-phase spots (corresponding to the four types of FE domains) arranged around the original PE-phase spot if h and k are both nonzero, so it is easy to note the coexistence of both types of spots. In the transition to the AFE phase, half the Bravais lattice points are lost, so a new set of Bragg spots appears. Also, each original Bragg spot divides into two spots on either side of the original spot, because the four types of AFE domains exist in pairs whose members cannot be distinguished by diffraction spot locations.

For mixed crystals of  $\text{Rb}_{1-x}(\text{NH}_4)_x\text{H}_2\text{AsO}_4$  (RADA) and its deuterated analog  $\text{Rb}_{1-x}(\text{ND}_4)_x\text{D}_2\text{AsO}_4$  (DRADA) with  $x$  below the range which prevents FE behavior, we have found that the spontaneous polarization  $P_s(x, T)$  along the crystalline  $\mathbf{c}$  axis does not rise sharply below a well-defined Curie temperature  $T_c$  (Pinto and Schmidt, 1993). Instead, it rises gradually with decreasing temperature (see Fig. 3). We consider that the ratio  $P_s(x, T)/P_s(0, 0)$  is the fraction  $f$  of FE material coexisting with the remaining PE material, namely

$$f(x, T) = P_s(x, T)/P_s(0, 0). \quad (1)$$

A competing hypothesis could be advanced in place of Eq. (1), namely that there is no coexistence, but instead that below  $T_c$  an entirely FE phase ( $f = 1$ ) has an unusual nearly linear increase of  $P_s$  as temperature decreases below  $T_c$ . We now present evidence against this hypothesis based on comparison of our  $P_s$  results with our measurements of dielectric permittivity  $\epsilon$  along the crystalline  $\mathbf{a}$  axis for RADA crystals in the  $x$  range from 0 to 0.20 (Trybula *et al.*, 1991).

We hypothesized (Pinto and Schmidt, 1993) that the fraction  $f$  of FE material equals the fraction of “missing” dielectric response;

$$f(x, T) = [\epsilon_{\text{pg}}(x_{\text{pg}}, T) - \epsilon_{\text{dc}}(x, T)]/[\epsilon_{\text{pg}}(x_{\text{pg}}, T) - \epsilon_{\infty}(0, 0)]. \quad (2)$$

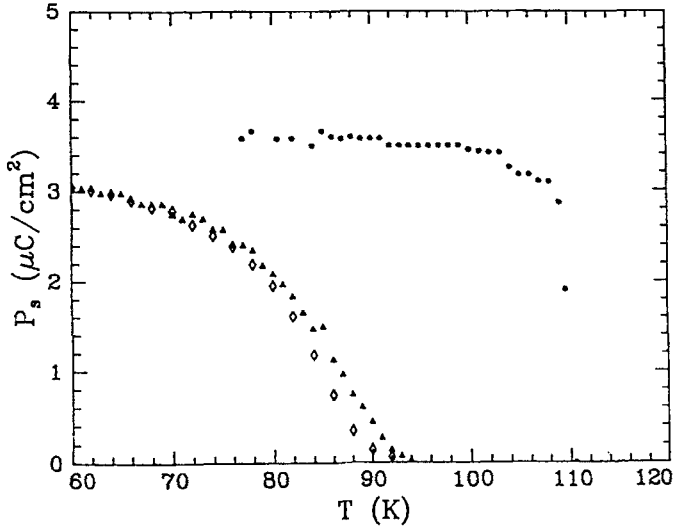


FIGURE 3 Spontaneous polarization (Pinto and Schmidt, 1993) obtained from hysteresis loops in RDA (solid circles) and  $x=0.08$  RADA (solid triangles). The open diamonds are obtained from dielectric permittivity measurements with the use of Eq. (2).

Here, the pg subscript refers to a crystal with  $x$  high enough to remain entirely in the PG phase at low temperature, and to a frequency low enough so that dielectric dispersion has not set in at temperature  $T$ . The dc subscript refers to the same low-frequency limit, but for the actual crystal of composition  $x$  under test. The  $\infty$  subscript refers to the  $a$  axis permittivity at audio frequencies of the FE ( $x=0$ ) parent crystal near 0 K, which only exhibits electronic and fast ionic response, but no audio-frequency dispersion or temperature dependence for temperatures well below  $T_c$ .

From these definitions, we see that the missing dielectric response  $\epsilon_{pg} - \epsilon_{dc}$  in the numerator of Eq. (2) is the response  $\epsilon_{pg}$  expected in the absence of FE-phase material, minus the low-frequency limit  $\epsilon_{dc}$  of the measured response, both plotted in Fig. 2. This missing response is compared to the maximum possible dielectric response from proton rearrangements in their hydrogen bonds,  $\epsilon_{pg} - \epsilon_{\infty}$ , which appears in the denominator of Eq. (2).

A brief explanation of Fig. 2 is now provided. We believe that the crystals of all four  $x$  values shown therein have the same true  $\epsilon_{\infty}$  value of  $11 \pm 1$ , and that the variations in  $\epsilon_{\infty}$  shown in Fig. 2 result from

errors in measuring crystal thickness and electrode area. Similarly, all four  $\epsilon_{\text{pg}}$  and  $\epsilon_{\text{dc}}$  curves have the same shape above  $T_c$  (the temperature range in which the  $\epsilon_{\text{pg}}$  and  $\epsilon_{\text{dc}}$  curves for a given  $x$  coincide). We extend the  $\epsilon_{\text{pg}}$  curves to 0 K for the  $x=0$ , 0.12, and 0.15 crystals using the same shape as exhibited by the  $x=0.20$  crystal which shows no FE transition.

After multiplying by numerical factors which bring these curves into coincidence and which give  $\epsilon_\infty = 11$  (typical for crystals of this family) for the  $x=0$  crystal, these curves obey a Curie–Weiss law

$$\epsilon_{\text{pg}} = \epsilon_\infty + C/(T - T_0), \quad (3)$$

where  $C = 16,000 \pm 1,000$  K and  $T_0 = -70 \pm 10$  K, for temperatures above 120 K. Below 120 K they flatten out and reach a value of  $110 \pm 10$  K at 0 K. The horizontal section deviates from the  $x=0.20$  crystal data at 1 Hz for temperatures below 35 K, but such a horizontal line was found by us for  $x=0.28$  DRADA in the dc limit in field cooling experiments (Pinto *et al.*, 1993b). The deviations below this common  $\epsilon_{\text{pg}}$  and  $\epsilon_{\text{dc}}$  line shown by the ac permittivity for the  $x=0.20$  crystal are typical of proton glass dispersion. Similar deviations occur below the  $\epsilon_{\text{dc}}$  lines for the  $x=0.12$  and 0.15 crystals, indicating that PG phase material remains well below  $T_c$ .

The  $\epsilon_{\text{dc}}$  curve for the  $x=0$  crystal goes quickly with decreasing temperature from the  $\epsilon_{\text{pg}}$  curve to the  $\epsilon_\infty$  line, with a rounded shape which is the mirror image of the spontaneous polarization curve (filled circles in Fig. 3). For the  $x=0.12$  and 0.15 crystals,  $\epsilon_{\text{dc}}$  stays above  $\epsilon_\infty$  even when approaching 0 K, indicating that these crystals never become completely FE. Even for very small  $x$ , nuclear quadrupole resonance (NQR) measurements (Papantopoulos *et al.*, 1994) show that some PG material remains at very low temperature.

We now return to consideration of the competing hypothesis that below  $T_c$  there is only a completely FE phase, with no coexistence. We see from Fig. 3 that Eqs. (1) and (2) give essentially the same temperature dependences for the product  $P_s(0, 0) f(0.08, T)$ . If there is no coexistence, then Eqs. (1) and (2) are incorrect, yet their right-hand sides must be equal, as seen from Fig. 3:

$$P_s(x, T)/P_s(0, 0) = [\epsilon_{\text{pg}}(x_{\text{pg}}, T) - \epsilon_{\text{dc}}(x, T)]/[\epsilon_{\text{pg}}(x_{\text{pg}}, T) - \epsilon_\infty(0, 0)]. \quad (4)$$

Such equality for all  $x$  and  $T$  for the left and right sides of Eq. (4), which relate to  $\mathbf{c}$  axis polarization and  $\mathbf{a}$  axis permittivity, would be a very unlikely coincidence. By equating both expressions to  $f(x, T)$ , the fraction of FE phase coexisting with the PE or PG phase, we obtain two equations, Eqs. (1) and (2), with simple and logical meanings, and have no need to invoke coincidences. Accordingly, we are convinced that phase coexistence is the only logical explanation for the above-described spontaneous polarization and dielectric permittivity phenomena.

Additional dielectric evidence for coexistence, in this case for AFE/PE coexistence in  $x=0.75$  RADP, comes from measurements by Takeshige *et al.* (1985), who at that time attributed the behavior to a reentrant phase diagram, going from PE to AFE to PG with decreasing temperature. The first mention of phase coexistence as the origin of such behavior (first a permittivity cusp, then dispersion at lower temperature) was by Trybula *et al.* (1991), in connection with FE/PE phase coexistence in RADA.

Nuclear magnetic resonance (NMR) provides additional evidence for coexistence. Kind *et al.* (1987) reported that in  $x=0.78$  DRADP the  $^{87}\text{Rb}$  NMR spectra of the PE and AFE phases overlap from 150 to 140 K. This to us implies phase coexistence, though they did not use this term. Later, Korner *et al.* (1993) presented a phase diagram for DRADP over the whole  $x$  range based on NMR results. This diagram shows a FE/PG phase segregation region, but they remarked that it is not clear whether such segregation is intrinsic or induced by defects. They also showed a region labeled AFE relaxor, which in our opinion could be a PE/AFE coexistence region.

Our NMR measurements of the deuteron spectrum and of the spin-lattice relaxation time  $T_1$  in  $x=0.10$  DRADA both demonstrate FE/PE coexistence in this deuteron glass (Pinto *et al.*, 1993a). Direct evidence for coexistence is seen in the  $\text{ND}_4^+$  rotationally-narrowed deuteron spectrum, in which a broad peak characteristic of the FE phase starts to appear near 138 K, while the two sharp peaks characteristic of the PE phase disappear near 131 K, as shown in Fig. 4.

Evidence for the length scale as well as the temperature range of this FE/PE coexistence in this DRADA crystal comes from  $T_1$  measurements for the  $\text{O}-\text{D}\cdots\text{O}$  deuterons. As temperature decreases, there is a downward  $T_1$  trend because of the slowing down of the fast intrabond deuteron motion. Superimposed on this downward trend,

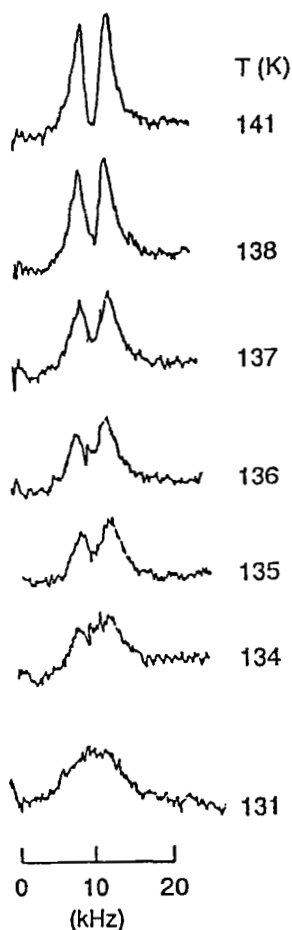


FIGURE 4 Temperature dependence of the  $\text{ND}_4^+$  deuteron NMR line shape (Pinto *et al.*, 1993a) in  $x=0.10$  DRADA for  $H_0 \parallel a$  at 28 MHz.

but only through the temperature range of onset of the FE phase,  $T_1$  increases because only the moving deuterons remaining in the PE phase contribute to spin-lattice relaxation. If these moving deuterons were independent of the “frozen” ones in the FE phase region, their  $T_1$  would still decrease. However, these deuterons are coupled by spin diffusion to the stationary deuterons in the FE phase, so their common  $T_1$  increases as fewer and fewer mobile deuterons must relax the entire deuteron spin system. The fact that they are coupled by spin diffusion

indicates that the correlation lengths for the FE and PE phases must be short, because otherwise spin diffusion could not achieve a common spin temperature for deuterons in the two phases. This  $T_1$  increase occurs in the range 138–125 K.

## **ANALYTICAL DESCRIPTION OF COEXISTENCE**

In systems without quenched spatial disorder, phase coexistence is usually considered to occur only in connection with critical fluctuations very near a second-order phase transition temperature, or right at a first-order transition temperature. An exception is semicrystalline polymers, because it is easy for some of the long molecules to align locally into crystals, but practically impossible for all the remaining amorphous material to align in this manner.

For crystals with quenched disorder, such as relaxor ferroelectrics and proton glasses, phase coexistence over an extended temperature range is possible in principle. Consider proton glasses, where the quenched disorder consists of random quenched placement of the ammonium and alkali cations. By chance, some regions will have higher concentrations of ammonium ions than adjacent regions. For small- $x$  crystals, these regions will resist transformation to the FE phase as temperature decreases, remaining in the PE phase. For large- $x$  crystals, such regions will transform first into the AFE phase, while other regions remain in the PE phase. Elastic forces will tend to counteract this tendency to separate into two phases having different unit cell shapes and sizes.

Is the resulting coexistence itself describable as quenched disorder? This question cannot be settled directly from experiments performed thus far. However, the answer can be found by considering, for example, the FE transition of RDA (RADA in the  $x=0$  limit). Some description of microscopic models for this transition is needed as background for answering the question. Slater (1941) developed the first explanation of the FE transition in  $\text{KH}_2\text{PO}_4$  (KDP) which is isomorphous to RDA. He postulated random off-center H positions above  $T_c$ , which order into a FE arrangement below  $T_c$ . This model predicted a step function change in polarization at  $T_c$ , from zero to a maximum value consistent with complete proton order.

A defect of the Slater model is that he allowed only six proton configurations around each phosphate ion, two protons close and two far, in the four H-bonds attached to the phosphate ion. Two of these  $\text{H}_2\text{PO}_4$  “Slater groups” are zero-energy polar groups corresponding to the two directions of FE polarization, while the other four are nonpolar and have higher energy  $\epsilon_0$ . This model leads to an order–disorder transition involving displacement of hydrogens from one off-center position to the other off-center position in the hydrogen bond. The problem is that if a hydrogen undergoes such motion, it creates a pair of  $\text{HPO}_4$  and  $\text{H}_3\text{PO}_4$  groups not allowed by the Slater model. Takagi (1947) remedied this problem by allowing such “Takagi groups” whose creation requires an energy  $\epsilon_1$ , typically about 5 times  $\epsilon_0$ . His model for the FE transition, including such groups, gave a second-order transition with  $P_s$  rising initially with infinite slope at  $T_c$ , then curving gradually toward  $P_{\text{sat}}$  as temperature decreases further. This result fit experiment much better than the Slater prediction of a  $P_s$  step function.

On the microscopic level, the “missing” polarization  $P_{\text{sat}} - P_s$  can be attributed to thermally generated  $\text{HPO}_4$ – $\text{H}_3\text{PO}_4$  Takagi pairs which then in effect diffuse apart within the FE domain by means of successive proton intrabond transfers. This diffusion leaves a chain of nonpolar Slater groups connecting the Takagi pair, thus lowering the polarization. At temperatures low enough so that these chains rarely cross, a model based on such chains reproduces the  $P_s(T)$  curve predicted by the Takagi model (Schmidt, 1961).

This dynamic process of pair creation, chain growth and decay, and pair recombination, first at one location and then another, is generally considered as part of the nature of the FE phase. For purposes of describing coexistence, it is preferable to consider these chains as PE inclusions. From this viewpoint, we say that the PE and FE phases coexist, but that this coexistence is “temporal” because the PE chains are as likely to be at one location as another.

At the other extreme, we consider a crystal with small but nonzero  $x$ , or with large but nonunity  $x$ , at low temperature such that some ordered FE or AFE phase coexists with the PE or PG phase. Upon approaching zero temperature this coexistence will be with the PG phase and will be quenched, so we can call this coexistence “spatial.” In general, for finite temperature and for  $x$  not equal to 0 or 1, the coexistence will be some combination of temporal and spatial.

It is desirable to describe the degree of coexistence, and the extent of its temporal and spatial natures, mathematically so that these parameters can be determined experimentally. For guidance, we consider the concept that each portion of a crystal must exist in some phase. For proton glass crystals, the volume fractions (and the respective phases) are  $f$  (FE),  $a$  (AFE),  $g$  (PG), and  $d$  (dynamic PE). (We use  $d$  instead of  $p$  for the PE phase because  $p$  denotes the FE order parameter;  $d$  is a reminder that the PE phase is the only dynamic phase of the four, while the rest are more or less static.) These four volume fractions must obey

$$f + a + g + d = 1. \quad (5)$$

To generalize this concept, we square both sides of the equation, giving

$$(f + a + g + d)^2 = 1. \quad (6)$$

Then we call terms such as  $f^2$  the FE autocorrelation parameter, and terms such as  $2fg$  the FE/PG coexistence parameter. In principle, proton glass crystals can exhibit six kinds of coexistence, but so far it appears that the FE/AFE parameter  $2fa$  is zero under all conditions.

To discuss these parameters, we need first to examine characteristics of the four phases and define the phase fractions  $f$ ,  $a$ ,  $g$ , and  $d$ . The FE and AFE phase regions are characterized by ordered hydrogen arrangements in the O–H $\cdots$ O or O–D $\cdots$ O bonds. The PG phase is characterized by a fixed disordered hydrogen arrangement in these bonds. The PE phase is characterized by dynamic disorder of hydrogens in these bonds. Accordingly, FE/PG or AFE/PG coexistence is completely spatial in nature, as would be FE/AFE coexistence if it were found to occur. Evidently, the PE phase is the vehicle for any hydrogen rearrangements. In order for boundaries between phases to shift, the PE phase must be involved, by means of temporal PE/FE, PE/AFE, or PE/PG coexistence.

Now we must describe how the *phase fractions*  $f$ ,  $a$ ,  $g$ , and  $d$  of the FE, AFE, PG, and PE phases are defined in terms of the various *order parameters* for the crystal. The order parameters are defined in terms of *pseudospins*, with  $S = 1$  corresponding to a proton off-center position in the O–H $\cdots$ O bond contributing to positive polarization along  $c$ ,

and  $S = -1$  for the other off-center position contributing to negative polarization. The order parameters  $O_j$  obey the relation

$$O_j = \langle S_j(0)S(t) \rangle, \quad (7)$$

where  $j$  refers to the type of order,  $\langle \rangle$  denotes the average over pseudospin sites,  $S_j$  is 1 or  $-1$  corresponding to the rule for the reference pseudospin at a given site at time zero, and  $S(t)$  is the actual pseudospin value at that site at time  $t$ . For the FE order parameter  $p$ , all the  $S_p$  are 1, corresponding to hydrogen positions for a positively polarized FE domain. The time values can be dropped from this definition ( $t=0$ ). For the AFE order parameters  $q$  and  $r$ , half the  $S_q$  and  $S_r$  are 1 and half are  $-1$ , corresponding to the hydrogen locations in the two respective reference domains. Again, time is irrelevant in this definition. For the Edwards–Anderson order parameter  $q_{\text{EA}}$ , the  $S_g(0)$  are the actual pseudospin values at  $t=0$ . For our use of  $q_{\text{EA}}$  in defining  $g$ ,  $t$  must approach infinity. The FE, AFE, and Edwards–Anderson order parameters are

$$\begin{aligned} \text{FE:} & \quad p = \langle S_p(0)S(0) \rangle = \langle S(0) \rangle, \\ \text{AFE:} & \quad q = \langle S_q(0)S(0) \rangle, \quad r = \langle S_r(0)S(0) \rangle, \\ \text{Edwards–Anderson:} & \quad q_{\text{EA}} = \langle S(0)S(\infty) \rangle. \end{aligned} \quad (8)$$

The phase fractions  $f$ ,  $a$ ,  $g$ , and  $d$  for the crystal are defined only indirectly in terms of the order parameters. The links between phase fractions and order parameters are the *cluster portions*  $f_c$ , etc. for clusters making up the crystal. The clusters are chosen to be small enough to be homogeneous, and large and compact enough so that their type of order is not due to random placement of hydrogens in their bonds. We will show below that the minimum cluster size is about 2 nm. The cluster portions are

$$\begin{aligned} \text{FE:} & \quad f_c = |p_c|, \\ \text{AFE:} & \quad a_c = |q_c| + |r_c|, \\ \text{PG:} & \quad g_c = q_{\text{EA}} - f_c - a_c \text{ or } 0, \text{ whichever is greater,} \\ \text{PE:} & \quad d_c = 1 - f_c - a_c - g_c. \end{aligned} \quad (9)$$

From these definitions, it is clear that a cluster should not contain substantial parts of two oppositely polarized FE domains; otherwise,

$f_c$  would underestimate the actual portion of FE material. The first definition for  $g_c$  takes into account that a static FE or AFE domain would contribute to  $q_{EA}$ . The second (zero) definition for  $g_c$  takes into account the possibility of FE or AFE clusters near a phase transition which are large enough to qualify as such clusters, but short-lived enough in their PE matrix so that they do not contribute to  $q_{EA}$ .

To maximize cluster homogeneity, with the aim of obtaining the best definitions for  $f$ ,  $a$ ,  $g$ , and  $d$ , we assign each cluster a nominal phase, corresponding to whichever of  $f_c$  etc. constitutes the largest portion for that cluster. We then find the fractional volumes  $v_f$ , etc. occupied by clusters of that nominal phase. We adjust the cluster boundaries, subject to the above compactness and minimum size criterion, to maximize the homogeneity parameter

$$H = v_f \langle f_{cf} \rangle + v_a \langle a_{ca} \rangle + v_g \langle g_{cg} \rangle + v_d \langle d_{cd} \rangle. \quad (10)$$

Here,  $\langle f_{cf} \rangle$  is the spatial average of  $f_c$  over all the nominally FE clusters, etc. There are only 4 terms in  $H$ , out of 16 possible terms which would add to unity. All 16 terms are needed in defining  $f$ ,  $a$ ,  $g$ , and  $d$ , which also must sum to unity. These definitions, for the volume fractions of the various phases for the entire crystal, are

$$\begin{aligned} f &= v_f \langle f_{cf} \rangle, \\ a &= v_a \langle a_{ca} \rangle, \\ g &= v_g (\langle g_{cg} \rangle + \langle f_{cg} \rangle + \langle a_{cg} \rangle) + v_f (\langle g_{cf} \rangle + \langle a_{cf} \rangle) + v_a (\langle g_{ca} \rangle + \langle f_{ca} \rangle), \\ d &= v_d (\langle d_{cd} \rangle + \langle f_{cd} \rangle + \langle a_{cd} \rangle + \langle g_{cd} \rangle) + v_f \langle d_{cf} \rangle + v_a \langle d_{ca} \rangle + v_g \langle d_{cg} \rangle. \end{aligned} \quad (11)$$

Table I illustrates the symmetry of this assignment of the 16 terms. There are several reasons for this assignment. First, a uniform electric field along  $\mathbf{c}$  in the PE phase would give a nonzero  $v_d \langle f_{cd} \rangle$  as the polarization response, but this must be counted as part of the PE phase, so it appears under  $d$  above. If the crystal is cooled in this field into the PG phase, this field-induced polarization then shows up in the  $v_g \langle f_{cg} \rangle$  term under  $g$ , because we do not consider the crystal to be at all FE, even though this polarization remains when the field is removed at low temperature (see discussion of field-cooling, zero-field-heating experiment below). Similarly, the  $v_d \langle g_{cd} \rangle$  term appears under  $d$  because the random bias field (caused by the two oxygens at opposite ends of the

TABLE I Assignment of cluster portion types to phases of the overall crystal

		Cluster Portion Type			
		FE	AFE	PG	PE
Cluster Type	FE	FE	negl.		
	AFE	negl.	AFE		
	PG			PG	
	PE				PE

hydrogen bond having different environments if one is close to an ammonium cation while the other is close to a rubidium cation) will give a nonzero Edwards–Anderson order parameter and corresponding nonzero  $g_{cd}$  even though the crystal is completely in the PE phase.

To summarize the phase assignments of Eq. (11) illustrated in Table I, the crystal is divided according to the above rules into clusters of four types, and each type has its own fractional volume. Each type of cluster has its own averaged values of the four cluster portions defined in Eq. (9). These sixteen averaged cluster portions, each multiplied by the appropriate fractional volume, form sixteen products which sum to unity. The assignment of these products to the four phases follows three rules:

- (1) The FE phase fraction  $f$  includes only the FE portions from the FE clusters; a similar rule holds for the AFE phase fraction  $a$ .
- (2) The PE phase fraction  $d$  includes all of the contents of the PE clusters, and the PE portions from all other types of clusters.
- (3) The PG phase fraction  $g$  contains everything else.

What form can these clusters take? One possibility is a FE cube-shaped cluster, whose minimum size is calculated below, in a PE matrix cluster composing the rest of the crystal. Another possibility is a Swiss-cheese-type PG cluster which percolates throughout the crystal, interlocked with a PE cluster which also percolates throughout the crystal. The above assignments allow for PE or PG phase inclusions (defined above as cluster portions) in FE or AFE domains (clusters), and for PE domain walls between oppositely polarized FE domains. Also, PE phase inclusions in PG clusters can occur.

Frequently, FE (or AFE) “clusters” are described in the literature as occurring in crystals with intermediate  $x$ , for which coexistence phenomena are not found. Even in an  $x=0$  FE crystal,  $\text{KH}_2\text{AsO}_4$ , quasistatic weakly polarized clusters have been observed (Blinic *et al.*, 1986). In our opinion, such “clusters” will not meet our FE cluster definition. If the region is large enough to be a cluster by our definition, it is probable that the polarization will be weak enough so that the majority portion of the cluster will be PE or PG, not FE. If the polarization is strong enough, it is probable that the size will be too small to qualify as a cluster, according to our example below for minimum size for a FE cluster.

To qualify as a FE region, a group of contiguous properly polarized  $\text{H}_2\text{PO}_4$  groups in a crystal of a given size must be larger than any such group that is likely to occur if the six types of  $\text{H}_2\text{PO}_4$  are placed randomly in the crystal, as they would be in the PE phase in the high-temperature limit. Consider how many cube-shaped clusters of  $n$  formula units can occur randomly in a crystal of  $N$  formula units. There are  $N$  origins for such a cluster. As a formula unit is added, in most cases it will have two polar neighbors specified, and it has a choice of one polar or one nonpolar hydrogen configuration. If only one such  $n$ -unit-size cluster is to occur randomly, we have the relation

$$N(1/2)^n = 1; \quad n = \ln(N)/\ln(2). \quad (12)$$

In a proton glass crystal 1 mm on a side,  $N$  is about  $10^{19}$  formula units, so  $n$  is about 64, corresponding to a cube somewhat under 2 nm on a side. This limiting size for a cluster to qualify as being FE depends only weakly on the crystal size, on the fact that clusters can have a variety of shapes, or on the fact that the cluster may not be composed entirely of like-polarized FE groups. For instance, if only half the groups in the cluster are FE, the cube side would increase to about 3 nm.

Similar minimum size requirements apply to AFE clusters. However, in accord with the definitions of Eq. (11) and Table I, there is no minimum size for a PE inclusion (or for the corresponding PG inclusion when it freezes at low temperature); it can be as small as an  $\text{HPO}_4\text{--H}_3\text{PO}_4$  pair embedded in a FE or AFE domain.

However, a PG cluster within a PE matrix must have a minimum size and compactness comparable to those of FE and AFE clusters, to insure that it is not by chance that this cluster of pseudospins did not

change sign with time. As temperature decreases in a crystal of intermediate  $x$  for which FE or AFE coexistence does not occur, such compact PG clusters will arise and will coalesce. If they are really PG clusters, their pseudospin arrangement is frozen in a local internal energy minimum, and this arrangement would be different if the crystal were heated and re-cooled. In other words, the onset of the PG phase is accompanied by the onset of nonergodicity. If these clusters arise because of freezing out of the configurations caused by the random bias field, then the configuration will not change after an annealing process. Experiments discussed in the next section, as well as Monte Carlo simulations, show that nonergodicity does occur.

There is not a sharp transition to the nonergodic PG phase. Perhaps there would be such a transition, as is seen for 3-d Ising spin glasses (Fischer and Hertz, 1991) in the absence of the random bias field. The situation may be analogous to that of a 2nd-order FE transition in a crystal such as RDP, which is smeared out by an electric field along the FE axis of the crystal. In any case, the proton glass crystal becomes nonergodic, and we follow usual practice in calling this the proton glass phase. However, we do not follow the common practice of defining a frequency-dependent transition temperature to the PG phase. We call such slowing down a pretransitional behavior.

## **DETERMINATION OF COEXISTENCE PARAMETERS**

First, for determination of the fractions of the various phases, the most direct way to find the FE fraction  $f$  is from the height of the hysteresis loop compared to its height for the parent ferroelectric crystal well below  $T_c$ , where  $P_s = P_{\text{sat}}$ . As mentioned above,  $f$  can also be found from dielectric measurements using Eq. (2), from NMR measurements, and (with some care) from neutron diffraction integrated intensities. To find the AFE fraction  $a$ , all of the above methods except hysteresis loops can be employed.

The PE and PG phases cannot be distinguished by an instantaneous view of the structure, even if it could be seen on the atomic scale. There is, however, a method called zero-field heating after field cooling, which provides this information. Upon removing a dc field after cooling to helium temperature where the crystal is completely

nonergodic and in the PG phase, there is a remanent polarization  $P_{ro}$ . It decays first slowly, and then quickly, to zero, upon heating the crystal slowly through the temperature at which it becomes completely ergodic and in the PE phase. The fraction  $g(T)$  of PG phase is given by

$$g(T) = P_r(T)/P_{ro}, \quad (13)$$

where  $P_r(T)$  is the remanent polarization at a given temperature  $T$ .

The basis of Eq. (13) is as follows. Glasses, spin glasses, and pseudospin glasses such as proton glasses have a multitude of states with internal energy near some minimum value. As the crystal is cooled, it will settle randomly into one of these states. In any given region of the crystal, various states with nearly the same energy will have considerably different configurations of hydrogen position  $S=1$  and  $S=-1$  pseudospins. In some regions these configurations have a positive polarization  $P$ , in other regions negative, but with zero applied field  $E$  the overall crystal will have zero  $P$ . If the crystal is cooled in a positive field, each region will prefer to settle into a state of positive  $P$ . When the field is removed at 4 K, even though some  $\text{HPO}_4$  and  $\text{H}_3\text{PO}_4$  bound charge carriers may still exist because they are trapped, they will not be able to migrate and change the polarization to zero. As temperature is raised, first some regions and then others can change their polarization (become locally ergodic and thus part of the PE phase). These regions will have zero polarization on the average, and cause the observed decline of polarization with rising temperature,  $P_r(T) = g(T)P_{ro}$ . Eventually the crystal will rise to the temperature  $T_g$  at which  $P=0$  and it becomes globally ergodic. The question is not settled as to whether  $T_g$  goes to 0 K as the experiment time is increased, but as a practical matter, changing the experiment time scale from seconds to hours has very little effect on  $T_g$ .

This experiment was first performed by Levstik *et al.* (1991) on  $x=0.60$  DRADP. Later it was done for  $x=0.28$  DRADA by Pinto *et al.* (1993b), who in addition performed a field heating after zero-field cooling experiment. In this case, application of a dc electric field at helium temperature produces a polarization  $P_i$  from the electrons and the ions in the absence of hydrogen rearrangement. With slowly increasing temperature,  $P_r(T)$  increases slowly at first, then rapidly to a maximum value  $P_f$ , after which it decreases slowly according to a

modified Curie–Weiss law. In this case, the fraction  $g$  of PG material is given by

$$g(T) = [P_f - P_r(T)]/[P_f - P_i]. \quad (14)$$

Both Eqs. (13) and (14) agreed on the temperature evolution of  $g$  as the respective experiments were performed for DRADA, as can be seen by examining Fig. 5.

Because these experiments were performed for  $x$  values between the two coexistence ranges, the paraelectric fraction was simply  $d = 1 - g$ . Similar cooling/heating experiments could be performed in the coexistence ranges of  $x$ . Then  $f$  or  $a$  would first be determined by one of the methods given above. The  $g$  values from Eqs. (13) or (14) would have to be multiplied by  $1 - f$  or  $1 - a$  to give the correct  $g$  values. This approach assumes that  $f$  and  $a$  no longer depend on  $T$  as the crystal approaches the ergodic limit temperature. Whether this assumption is correct can be determined by whether the lowest-frequency permittivity curves flatten out above this temperature. (There is still controversy on

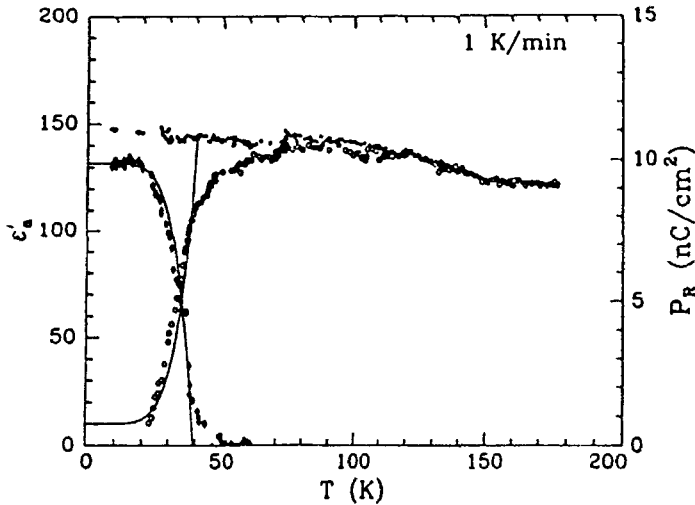


FIGURE 5 Temperature dependence of the field-heated (open circles), field-cooled (solid circles, and zero-field-heated (open diamonds) polarization (Pinto *et al.*, 1993b) in  $x = 0.28$  DRADA. A field of 500 V/cm was applied along the  $a$  axis, and the heating and cooling rates were 1 K/min. The  $a$  axis permittivity scale has meaning in the ergodic region above 50 K. Solid lines represent fits to a theory described in the above reference.

whether there is a real ergodic limit, or only a practical one based on time which can be devoted to the experiment.)

For determination of the Edwards–Anderson order parameter,

$$q_{EA} = \langle S(0)S(t) \rangle, \quad (15)$$

2d NMR is an ideal technique and has been employed by Blinc *et al.* (1994) in DRADP to study the freezing out of deuteron intrabond motion with decreasing temperature in this deuteron glass. This technique directly determines what fraction of deuterons in a given type of site at  $t = 0$  are still in that site at a later time  $t$ , that is, it finds  $\langle q_{EA} \rangle$  averaged over that type of site.

A similar technique could find the spatial coexistence parameter  $\langle s(x, T, t) \rangle$  for coexistence of FE and PE phases. One could select a subset of FE phase deuterons with a certain electric field gradient tensor orientation to observe at  $t = 0$ . In a 2-d NMR experiment, these deuterons could be allowed to mix with a subset of PE phase deuterons. If the volume fraction are  $f$  and  $d$  for the FE and PE phases, with  $f + d = 1$ , then for complete mixing (temporal coexistence) one would obtain  $q_{EA} = f$ . For no mixing (spatial coexistence) one would obtain  $q_{EA} = 1$ . Then the degree to which the coexistence is spatial is given by

$$\langle s(x, T, t) \rangle = [q_{EA}(t) - f] / [1 - f], \quad (16)$$

where the  $\langle \rangle$  indicate a spatial average over initially FE sites, because  $q_{EA}$  will vary from site to site because of the random distribution of rubidium and ammonium ions. Similar experiments could determine  $s(x, T, t)$  for AFE/PE coexistence.

Neutron diffraction provides a method of finding the fractions  $f$  or  $a$  of FE or AFE phase material coexisting with the PE and/or PG phase. Neutron diffraction will only detect a cluster of a certain size with the FE or AFE cluster, comparable to the minimum size for our definition of a FE or AFE cluster. Care is needed in determining the amount of FE, AFE or disordered (PE or PG) material present from the area under diffraction peaks.

Another approach to examine questions of ergodicity, phase coexistence, and response rate which we have used is Monte Carlo stochastic-dynamics simulations (Sinitski and Schmidt, 1996). These

have yielded results, for instance, in good accord with the field cooling and field heating experiments.

Once the fractional amounts of phases  $f$ ,  $a$ ,  $g$ , and  $d$  are determined, it is possible also to determine auxiliary parameters such as the coexistence parameters  $2fd$ , etc., discussed in connection with Eq. (6). Another auxiliary parameter, discussed above, is the fraction  $s$  of static coexistence of an ordered phase (FE or AFE) with a disordered phase. All these parameters can be plotted on  $x$ - $T$  phase diagrams, as discussed below.

## CONCLUSIONS

We have proposed nomenclature and expressions for representing analytically the fractions of coexisting phases, and the degree to which their coexistence is spatial or temporal. Our example system is proton glass, for which we define fractional volumes  $f$ ,  $a$ ,  $g$ , and  $d$  for the ferroelectric, antiferroelectric, paraelectric, and proton glass phases respectively. The ideas can be extended to other systems, such as relaxor ferroelectrics, with quenched structural features which give rise to phase coexistence. We have shown how some of these coexistence parameters have already been measured, and have indicated how other ones could be determined.

For systems with coexistence, typical  $x$ - $T$  phase diagrams such as in Fig. 1 are inadequate. One could show contours on such diagrams of constant fractions such as  $f=0.9$ , etc. for the various phases. Contours of constant spatial coexistence parameter  $s(x, T)$  could also be shown. Finally, contours of the overall coexistence parameter

$$c = 2fa + 2fg + 2ag + 2fd + 2ag + 2gd \quad (17)$$

could be plotted. The ridge lines of these contours could be called the nominal phase boundaries, keeping in mind that with coexistence the boundaries are smeared out.

Numerous problems remain, such as determination of the spatial nature (correlation length, shape) of coexisting phases. Also, existing data should be plotted on contour-map-type phase diagrams as suggested above, and additional data should be accumulated to fill in what would be the large blank spaces on such diagrams.

## Acknowledgement

This work was supported in part by NSF Grant DMR-9520251.

## References

- Blinc, R., J. Dolinšek, B. Zalar and F. Milia (1994). Proton and deuteron glasses – 1d and 2d NMR and NQR. *J. Non-Cryst. Solids* **172**, 436.
- Blinc, R., M. Koren, J. Slak, V. Rutar, S. Žumer and J.L. Bjorkstam (1986). Cluster distribution in paraelectric  $\text{KH}_2\text{AsO}_4$ . II.  $^{75}\text{As}$  spin–spin and spin–lattice relaxation. *Phys. Rev. B* **34**, 3112.
- Courtens, E. (1982). Competing structural orderings and transitions to glass in mixed crystals of  $\text{Rb}_{1-x}(\text{NH}_4)_x\text{H}_2\text{PO}_4$ . *J. de Physique* **43**, L-109.
- Courtens, E. (1987). Mixed crystals of the  $\text{KH}_2\text{PO}_4$  family. *Ferroelectrics* **72**, 229.
- Jona, F. and G. Shirane (1962). *Ferroelectric Crystals*, Macmillan, New York, pp. 63–107.
- Fischer, K.H. and J.A. Hertz (1991). *Spin Glasses*, Cambridge, p. 375.
- Känzig, W. (1957). Ferroelectrics and Antiferroelectrics. In F. Seitz and D. Turnbull (Eds.), *Solid State Physics*, Vol. 4, Academic, New York, pp. 124–180.
- Kind, R., O. Liechti, R. Brüscheiler, J. Dolinšek and R. Blinc (1987).  $^{87}\text{Rb}$  NMR study of the paraelectric–antiferroelectric phase transition in  $\text{Rb}_{0.22}(\text{ND}_4)_{0.78}\text{D}_2\text{PO}_4$ . *Phys. Rev. B* **36**, 13.
- Korner, N., Ch. Pfammatter and R. Kind (1993). Soft mode, “relaxor,” and glassy-type dynamics in the solid solution  $\text{Rb}_{1-x}(\text{ND}_4)_xD_2\text{PO}_4$ . *Phys. Rev. Lett.* **70**, 1283.
- Levstik, A., C. Filipič, Z. Kutnjak, I. Levstik, R. Pirc, B. Tadić and R. Blinc (1991). Field-cooled and zero-field-cooled dielectric susceptibility in deuteron glasses. *Phys. Rev. Lett.* **66**, 2368.
- Papantopoulos, G., G. Papavassiliou, F. Milia, V.H. Schmidt, J.E. Drumheller, N.J. Pinto, R. Blinc and B. Zalar (1994).  $^{75}\text{As}$  nuclear quadrupole resonance in weakly substitutionally disordered  $\text{Rb}_{1-x}(\text{NH}_4)_x\text{H}_2\text{AsO}_4$ . *Phys. Rev. Lett.* **73**, 276.
- Pinto, N.J., F.L. Howell and V.H. Schmidt (1993a). Deuteron NMR study of dynamics and of coexistence of paraelectric and ferroelectric phases in  $\text{Rb}_{0.90}(\text{ND}_4)_{0.10}\text{D}_2\text{AsO}_4$ . *Phys. Rev. B* **48**, 5983.
- Pinto, N.J., K. Ravindran and V.H. Schmidt (1993b). Field-heated, field-cooled, and zero-field-heated static permittivity of the deuteron glass  $\text{Rb}_{1-x}(\text{ND}_4)_xD_2\text{AsO}_4$ . *Phys. Rev. B* **48**, 3090.
- Pinto, N.J. and V.H. Schmidt (1993). Spontaneous polarization in the deuterated and undeuterated proton glass  $\text{Rb}_{1-x}(\text{NH}_4)_x\text{H}_2\text{AsO}_4$ . *Ferroelectrics* **141**, 207.
- Schmidt, V.H. (1961). Deuteron jumping in  $\text{KH}_2\text{PO}_4$ . Ph.D. Thesis, University of Washington, pp. 90–91.
- Schmidt, V.H. (1987). Review of order–disorder models for KDP-type crystals. *Ferroelectrics* **72**, 157.
- Schmidt, V.H., D.L. Brandt and S.M. Shapiro (1996). Neutron diffraction study of phase coexistence and transitions in DRADA deuteron glass crystals. *Bull. Am. Phys. Soc.* **41**, 167 (a detailed account is in preparation).
- Sintiski, A. and V.H. Schmidt (1996). Monte Carlo stochastic-dynamics study of dielectric response and nonergodicity in proton glass. *Phys. Rev. B* **54**, 842.
- Slater, J.C. (1941). Theory of the transition in  $\text{KH}_2\text{PO}_4$ . *J. Chem. Phys.* **9**, 16.
- Takagi, Y. (1947). Theory of the transition in  $\text{KH}_2\text{PO}_4$  (II). *J. Phys. Soc. Jpn.* **3**, 273.
- Takeshige, M., H. Terauchi, Y. Miura, S. Hoshino and T. Nakamura (1985). Dielectric dispersion of  $\text{Rb}_{1-x}(\text{NH}_4)_x\text{H}_2\text{PO}_4$ . *Jpn. J. Appl. Phys.* **24**, Suppl. 24–2, 947.
- Trybula, Z., V.H. Schmidt and J.E. Drumheller (1991). Coexistence of proton-glass and ferroelectric order in  $\text{Rb}_{1-x}(\text{NH}_4)_x\text{H}_2\text{AsO}_4$ . *Phys. Rev. B* **43**, 1287.